



COVER SHEET

This is the author-version of article published as:

Frost, Ray and Reddy, Jagannadha (2006) Thermo-Raman spectroscopic study of the natural layered double hydroxide manasseite. *Spectrochimica Acta* 65(3-4):pp. 553-559.

Copyright 2006 Elsevier

Accessed from <http://eprints.qut.edu.au>

Thermo-Raman spectroscopic study of the natural layered double hydroxide manasseite

Ray L. Frost* and B. Jagannadha Reddy

Inorganic Materials Research Program, School of Physical and Chemical Sciences, Queensland University of Technology, GPO Box 2434, Brisbane Queensland 4001, Australia.

Abstract

Raman and thermo-Raman spectroscopy have been applied to study the natural hydrotalcite manasseite $\text{Mg}_6\text{Al}_2(\text{OH})_{16}(\text{CO}_3)\cdot 4\text{H}_2\text{O}$. Hydrogen bond distances calculated using a Libowitzky-type empirical function varied between 2.61 and 3.00 Å. Stronger hydrogen bonds were formed by water units as compared to the hydroxyl units. Thermo-Raman spectroscopy enabled the identification of bands attributed to the hydroxyl units. Two Raman bands at 1062 and 1058 cm^{-1} are assigned to symmetric stretching modes of the carbonate anion. Thermal treatment shifts these bands to higher wavenumbers indicating a change in the carbonate bonding.

Keywords: Manasseite; Sjögrenite; Stichtite; Iowaite; Desautelsite; Takovite; Hydrotalcite; Raman spectroscopy

1. Introduction

Studies of anionic clays have been undertaken for a long time [1-3]. Anionic clays, hydrotalcites or layered double hydroxides (LDH) are less well-known than cationic clays like smectites [4-6]. The structure of hydrotalcite can be derived from a brucite structure ($\text{Mg}(\text{OH})_2$) in which e.g. Al^{3+} or Fe^{3+} (pyroaurite-sjögrenite) substitutes a part of the Mg^{2+} . This substitution creates a positive layer charge on the hydroxide layers, which is compensated by interlayer anions or anionic complexes. In hydrotalcites a broad range of compositions are possible of the type $[\text{M}^{2+}_{1-x}\text{M}^{3+}_x(\text{OH})_2][\text{A}^{n-}]_{x/n}\cdot y\text{H}_2\text{O}$, where M^{2+} and M^{3+} are the di- and trivalent cations in the octahedral positions within the hydroxide layers with x normally between 0.17 and 0.33. A^{n-} is an exchangeable interlayer anion. Many variations in compositions have been reported for hydrotalcites [4, 7-12]. Two types of structures exist depending upon whether the crystallography is trigonal or hexagonal. The trigonal groups are known as the hydrotalcites whereas the hexagonal carbonates form the manasseite group. One of the variations in cations of hydrotalcite comprises takovite in which Mg is replaced by Ni. The hexagonal equivalent is manasseite.

The manasseite groups of minerals are hexagonal carbonates similar to the triclinic carbonates known as the hydrotalcites or double layer hydroxides [13-16]. Manasseite is the mineral $\{\text{Mg}_6\text{Al}_2(\text{OH})_{16}\text{CO}_3\cdot 4\text{H}_2\text{O}\}$ and is related to the mineral sjögrenite by replacement of trivalent Al with trivalent Fe. Other members of the group are chloromagaluminite [17] in which the Mg is replaced with some divalent Fe and barbertonite in which the Al is replaced with trivalent Cr. This mineral has an identical formulation to stichtite except the structure is hexagonal and may be

* Author to whom correspondence should be addressed (r.frost@qut.edu.au)

considered as a polymorph of stichtite. In this work we report the Raman spectrum of manasseite and relate the spectrum to the structure of the mineral. Thermo-Raman spectroscopy has been applied to study the thermal stability of the mineral and to determine Raman bands due to water vibrations. The Raman data is complimented by data obtained from infrared spectroscopy.

2. Experimental

2.1 The Manasseite Mineral

The mineral manasseite was supplied by Museum Victoria and originated from Nordmark, Filipstad, Värmland, Sweden. The mineral was analysed by X-ray diffraction for phase purity and by SEM-EDAX analysis for chemical composition.

2.2 Raman microprobe spectroscopy

The crystals of manasseite were placed and orientated on a polished metal surface on the stage of an Olympus BHSM microscope, which is equipped with 10x and 50x objectives. The microscope is part of a Renishaw 1000 Raman microscope system, which also includes a monochromator, a filter system and a Charge Coupled Device (CCD). Raman spectra were excited by a Spectra-Physics model 127 He-Ne laser (633 nm) at a resolution of 2 cm^{-1} in the range between 4000 and 100 cm^{-1} . Repeated acquisition, using the highest magnification, was accumulated to improve the signal to noise ratio in the spectra. Spectra were calibrated using the 520.5 cm^{-1} line of a silicon wafer. Powers of less than 1 mW at the sample were used to avoid laser induced degradation of the sample [18-20]. Slight defocusing of the laser beam also assists in the preservation of the sample.

Spectra at elevated temperatures were obtained using a Linkam thermal stage (Scientific Instruments Ltd, Waterfield, Surrey, England).

2.3 Infrared Spectroscopy

Infrared spectra were obtained using a Nicolet Nexus 870 FTIR spectrometer with a smart endurance single bounce diamond ATR cell. Spectra over the $4000\text{--}525\text{ cm}^{-1}$ range were obtained by the co-addition of 64 scans with a resolution of 4 cm^{-1} and a mirror velocity of 0.6329 cm/s .

Spectroscopic manipulation such as baseline adjustment, smoothing and normalisation were performed using the Spectracalc software package GRAMS (Galactic Industries Corporation, NH, USA). Band component analysis was undertaken using the Jandel 'Peakfit' software package, which enabled the type of fitting function to be selected and allows specific parameters to be fixed or varied accordingly. Band fitting was done using a Gauss-Lorentz cross-product function with the minimum number of component bands used for the fitting process. The Lorentz-Gauss ratio was maintained at values greater than 0.7 and fitting was undertaken until reproducible results were obtained with squared correlations of R^2 greater than 0.995.

3. Results and discussion

3.1 Raman and infrared spectroscopy of the hydroxyl stretching region

One way of looking at hydrotalcites is to consider the molecules to be giant cations with a distribution of positive charges over the surfaces. These charges may be random or in some regular array. The positive charges must be counterbalanced by anions such as carbonate. The carbonate anions are hydrated and these hydrated anions together with water in some structured arrangements completely fill the interlayer of manasseite. The brucite-like surface will attract the anions and water molecules hydrogen bonded to the brucite-like surface. Thus in any vibrational spectroscopic analysis of manasseite each vibrational species will be observed. One of the difficulties of obtaining the infrared spectra of hydrotalcites is the overlap of the water hydroxyl stretching bands with those of hydroxyls bound to metal centres. The infrared absorption of water is so intense that the hydroxyl absorption bands of the metal hydroxides are difficult to detect. Water is a very poor Raman scatterer and so Raman microscopy is more useful for the measurement of the OH stretching region of the M_3OH units for the study of hydrotalcites.

In brucite type solids, there are tripod units M_3OH with several metals such as M, M', M''. In hydrotalcites such as those based upon Mg and Zn of formula $Mg_xZn_{6-x}Al_2(OH)_{16}(CO_3).4H_2O$, a number of statistical permutations of the M_3OH units are involved. These are Mg_3OH , Zn_3OH , Al_3OH and combinations such as Mg_2ZnOH , Zn_2MgOH , Mg_2AlOH , Al_2MgOH , Al_2ZnOH , Zn_2AlOH , and even $MgZnAlOH$. These types of units will be distributed according to a probability distribution based on the composition. In this model, a number of assumptions are made, namely that the molecular assembly is random and that no islands or lakes of cations are formed. Such an assembly is beyond the scope of this work but needs to be thoroughly investigated. In the simplest case namely $Mg_6Al_2(OH)_{16}(CO_3).4H_2O$ the types of units would be Mg_3OH , Mg_2AlOH , $MgAl_2OH$ and Al_3OH . A similar situation would exist for the $Zn_6Al_2(OH)_{16}(CO_3).4H_2O$ hydrotalcite. In a somewhat over simplified model, for the $Mg_6Al_2(OH)_{16}(CO_3).4H_2O$ hydrotalcite, the most intense bands would be due to the Mg_2AlOH based upon an Al:Mg ratio of 1:3 followed by Mg_3OH and Al_3OH units.

The infrared and Raman spectra in the hydroxyl stretching region are shown in Fig. 1. The results of the Raman and infrared spectral analyses are reported in Table 1. The spectral profile is broad and it is unlikely that there will be any unique solution for any band component analysis of the infrared and Raman profiles. However it is useful to determine the bands in the spectral profiles [21, 22]. This technique enables a study of the bands and their possible assignments. The Raman spectrum of manasseite does show more features than the infrared counterpart. Raman bands are observed at 3589, 3491, 3386, 3255, 3060 and 2930 cm^{-1} . The bands are broad and the width varies from 70 to 328 cm^{-1} . The first band at 3589 cm^{-1} with a band width approximately 50% less than the other bands may be attributed to the OH stretching from the brucite-like surface [9, 23-31]. Previous studies have identified bands in these positions to the OH stretching vibrations [9, 23-31]. In the infrared spectrum a series of bands are observed at 3553, 3456, 3386, 3240, 3036, 2845 and 2681 cm^{-1} . The infrared bands are broader than the equivalent Raman bands.

An empirical relationship has been developed for the variation of hydrogen bond distances and infrared spectroscopic wavenumbers [32]. Studies have shown a strong correlation between OH stretching frequencies and both O···O bond distances and H···O hydrogen bond distances [33-36]. Libowitzky (1999) showed that a regression function can be employed relating the hydroxyl stretching frequencies with regression coefficients better than 0.96 using infrared spectroscopy [37]. The function is described as: $\nu_1 = (3592 - 304) \times 109^{\frac{-d(O-O)}{0.1321}} \text{ cm}^{-1}$. Thus OH---O hydrogen bond distances may be calculated using the Libowitzky empirical function [32]. The infrared bands listed above hence provide estimates of hydrogen bond distances of 3.00, 2.843, 2.78, 2.71, 2.65 and 2.61 Å. The significance of these results rests with their interpretation. The hydrogen bond distances may be divided into two groups (a) those above 2.70 Å and those below 2.70 Å. Such a division is entirely arbitrary but serves to differentiate bonds which may be regarded as stronger hydrogen bonds (group b) as opposed to weaker hydrogen bonds as with group a. The stronger hydrogen bonds are formed with the bonding involving the water molecules.

The thermo-Raman spectra of the hydroxyl stretching region are displayed in Fig. 2. Spectra are shown at 25, 50, 100, 150 and 200 °C. A number of conclusions can be made (a) the water in the interlayer is retained up to 150 °C (b) the loss of water forces the carbonate to bond with the hydroxyl units. This is observed by the band at 2970 cm⁻¹ at 25 °C, 2950 cm⁻¹ at 50 °C, 2920 cm⁻¹ at 100 and 2924 cm⁻¹ at 150 °C. The band is not observed in the 200 °C spectrum. It is likely the bonding of the carbonate to the interlayer water is destroyed at the elevated temperature and the carbonate is forced to bond with the hydroxyl layer. In addition bands are observed at 3600 cm⁻¹ (25 °C), 3587 cm⁻¹ (50 °C), 3660 cm⁻¹ (100 °C) 3610 cm⁻¹ (150 °C) and 3742 cm⁻¹ (200 °C). These bands are assigned to the OH stretching bands of the hydroxyl units of the brucite-like layer. It is probable that all the bands in the 200 °C spectrum at 3742, 3637, 3600, 3546 and 3450 cm⁻¹ are attributable to hydroxyl unit stretching vibrations (top spectrum in Fig. 2).

3.2 Raman and infrared Spectroscopy of the 1800 to 1100 cm⁻¹ region

The unperturbed carbonate ion is a planar triangle with point symmetry D_{3h} . Group theoretical analysis of the carbonate ion predicts four normal modes the ν_1 symmetric stretch of A_1' symmetry normally observed at 1063 cm⁻¹, the anti-symmetric stretch of E' symmetry observed at 1415 cm⁻¹, the ν_2 out of plane bend at 879 cm⁻¹ and the in-plane bend at 680 cm⁻¹. For the unperturbed carbonate anion the ν_1 mode is Raman active only. For the perturbed carbonate anion, all modes are both Raman and infrared active except for the ν_2 mode, which is IR active only.

The Raman and infrared spectra of the 1800 to 1100 cm⁻¹ region of manasseite are shown in Fig. 3. The results of the Raman spectral analysis are given in Table 1. The Raman spectrum of manasseite is simple in this region with a single band observed at 1404 cm⁻¹ with a band width of 39.0 cm⁻¹. This band is assigned to the ν_3 antisymmetric stretching vibration. The infrared spectrum is complex with three bands observed at 1403, 1356 and 1346 cm⁻¹. One possible interpretation is that these bands are attributable to the carbonate anion in different environments. Three environments are possible (a) free carbonate anion (b) water hydrogen bonded

carbonate anion and (c) hydroxyl bonded carbonate anion from the brucite-like surface. A number of infrared bands are observed at 1750, 1634, 1512, 1447 and 1403 cm^{-1} . The first band may be attributed to the HOH bending mode of the interlayer water. The other bands may be due to hydroxyl deformation modes of Al and perhaps Mg.

3.3 Raman and infrared Spectroscopy of the 1100 to 900 cm^{-1} region

The Raman spectrum of manasseite in the 1100 to 900 cm^{-1} region is shown in Fig. 4. Two bands are observed at 1062 and 1058 cm^{-1} and are very sharp. These two bands are assigned to the ν_1 symmetric stretching mode of the carbonate anion. In this type of hydroxylite there are two types of OH units, namely Al_3OH and Mg_3OH . It is questionable whether band fitting could resolve two bands at 2 cm^{-1} nominal resolution of the Renishaw spectrometer. One most likely model is that the 1062 cm^{-1} band is attributable to carbonate associated with the Al_3OH unit and the 1058 cm^{-1} band with Mg_3OH unit. The Raman spectrum of magnesite (MgCO_3) displays a band at 1087 cm^{-1} (this work). Thus the behavior of the carbonate ion in the hydroxylites is more like that of a perturbed carbonate ion rather than a carbonate bonded to the cation. The observation of two bands supports the concept of two types of carbonate anions. Two other bands are observed at 1035 and 958 cm^{-1} attributed to water librational modes. The symmetric stretching mode of smithsonite (ZnCO_3) is observed at 1093 cm^{-1} (this work). This result again suggests that the carbonate is not bonded to any of the cations and although perturbed by hydrogen bonding with water free from cations. It is possible that water acts as a donor acceptor and forms a bridging unit between the M_3OH units and the carbonate anion.

The thermo-Raman spectrum of manasseite is shown in Fig. 5. Two bands are observed in the 50 and 100 $^\circ\text{C}$ spectra at ~ 1060 and 950 cm^{-1} . The former band shifted to higher wavenumber whilst the latter disappeared in the 150 $^\circ\text{C}$ spectrum. This observation confirms the assignment of these bands to water librational modes. In the 50 $^\circ\text{C}$ spectrum two bands are observed at 1079 and 1060 cm^{-1} . These bands are ascribed to the symmetric stretching mode of two carbonate anions, one bonded to the hydroxyl surface and another to interlayer water. At 100 $^\circ\text{C}$, the intensity of the 1078 cm^{-1} increased and the 1065 cm^{-1} band decreased showing the carbonate anion bonded to the hydroxyl surface increases as the amount of water is lost. In the spectra at 150 and 200 $^\circ\text{C}$ the band at 1065 cm^{-1} observed in the 100 $^\circ\text{C}$ is shifted to lower wavenumbers and additional bands at 1097 cm^{-1} (100 $^\circ\text{C}$) and 1104 cm^{-1} (200 $^\circ\text{C}$) are observed. The band at 1065 cm^{-1} shifts to higher wavenumbers with increasing temperature. This band may be assigned to the carbonate anion bonded to the hydroxyl brucite like surface. The infrared spectrum in the 1050 to 550 cm^{-1} region is shown in Fig. 6. The infrared spectrum of this region shows two bands at 968 and 937 cm^{-1} . These bands are ascribed to water librational modes.

3.4 Raman and infrared Spectroscopy of the 850 to 250 cm^{-1} region

The Raman spectrum of the 850 to 250 cm^{-1} region is shown in Fig. 7. The infrared spectrum in this region is very limited because of the cut-off point of the diamond ATR cell at 550 cm^{-1} . Thus only bands above this wavenumber can be measured using this technique. The ν_2 out of plane bend is difficult to observe for this hydroxylite. For MgCO_3 of calcite structure ν_2 is observed as a band at 892 cm^{-1} (this

work). The ν_2 bending mode varies depending upon the cation from 862 to 892 cm^{-1} . This ν_2 bending mode is observed at 870 cm^{-1} in the infrared spectrum as a shoulder on the intense 779 cm^{-1} band (Fig. 6). This band is not observed in the Raman spectrum. Two infrared bands are observed at 660 and 632 cm^{-1} . These bands may also be additional ν_4 modes ascribed to the different carbonate anions in the manasseite structure. A broad low intensity band centred upon 817 cm^{-1} is observed. The ν_4 mode is observed in the Raman spectrum at 696 cm^{-1} with a component at 692 cm^{-1} and is shown in Fig. 7. For manasseite an intense infrared band is observed at 779 cm^{-1} with a shoulder on either side at 818 and 752 cm^{-1} . These bands are assigned to ν_4 bending modes. The observation of more than one band is indicative of a reduction in symmetry. The carbonate hydrogen bonding to a water molecule in the interlayer could envisage such a reduction. Alternatively the carbonate might bond to one of the surface hydroxyl units.

A very intense Raman band is observed at 556 cm^{-1} . The band observed at 556 cm^{-1} is the second most intense band in the hydrotalcite spectra and is polarised. The intensity of this band infers that it is due to a symmetric stretching vibration. One possibility is that the band originates from the carbonate-water unit. The two hydrogens of the H_2O molecule are bridged to the two oxygens of the $(\text{CO}_3)^{2-}$ anion. The 556 cm^{-1} band appears to be unique to the hydrotalcite structure. It is proposed that this band is a result of OH—O units formed as a result of the water bonding to the carbonate anion. Such a concept is supported by the infrared spectrum of the ν_3 region where splitting is observed with some 30 cm^{-1} difference. This means the symmetry of the carbonate has been reduced from D_{3h} to C_{2v} .

The proposed model of carbonate anion in manasseite is of C_{2v} symmetry. The Mg_3OH deformation mode is observed at 958 cm^{-1} but is very weak. The Al_3OH deformation mode is probably around 1035 cm^{-1} but is masked by the intense $(\text{CO}_3)^{2-}$ stretching modes of the carbonate at 1058 and 1062 cm^{-1} . Bands at 1035 cm^{-1} are observed in mineral such as boehmite ($\text{AlO}(\text{OH})$). The Raman spectrum of brucite shows an intense band at 442 cm^{-1} . The equivalent band in the spectrum of manasseite is around 474 cm^{-1} depending on the degree of cation substitution. This band is assigned to the MgO symmetric stretching vibration. For the formation of synthetic Mg_4Zn_2 hydrotalcite two bands are observed in this region at 481 and 467 cm^{-1} . The band is centred on 491 cm^{-1} for the synthetic Zn_6 hydrotalcite. A band is also observed in brucite at 396 cm^{-1} . Bands are observed at ~ 396 , 362 and 302 cm^{-1} in the Raman spectrum of manasseite. Such bands have been observed for other layered double hydroxides in these positions. These bands are attributed to the OMO bending modes. It is interesting that hydrotalcite of formula $[\text{Mg}_6\text{Al}_2(\text{OH})_{16}\text{CO}_3 \cdot 4\text{H}_2\text{O}]$ is triclinic. Manasseite is also of the same formula; yet the structure is hexagonal. The Raman bands of hydrotalcite and manasseite are in similar positions for both minerals.

4. Conclusions

Insight into the unique structure of hydrotalcites has been obtained using a Raman microscope. The hydroxyl-stretching units of Al_3OH , Mg_3OH , and Zn_3OH are identified by unique band positions. Water plays a unique role in the stabilisation of the hydrotalcite structure. The position and intensity of the Raman bands in the hydroxyl-stretching region indicates that the water is highly structured. The position

of the bands in the hydroxyl deformation region of the infrared spectrum supports the concept of structured water between the hydrotalcite layers. Four types of water are identified (a) water hydrogen bonded to the interlayer carbonate ion (b) interlamellar water (c) water hydrogen bonded to the hydroxyl units (d) water which bridges the carbonate anion and the M_3OH surface. The position of the suite of bands associated with the carbonate ion indicates the carbonate ion is perturbed and not bonded to the metal centres but is strongly hydrogen bonded to the interlayer water. An intense band at around 550 cm^{-1} is observed and it is proposed that this band is due to the librational mode of water hydrogen bonded to the metal hydroxyl surface.

In this work, the Raman spectra of the interlayer anions of carbonate of a natural mineral (manasseite) have been collected. The splitting of the ν_3 , ν_4 and ν_2 modes indicates symmetry lowering. The symmetry lowering must be taken into account through the bonding of carbonate anion to both water and the brucite-like hydroxyl surface. Water plays an essential role in the hydrotalcite structure as may be evidenced by the position of the water bending modes. The water is strongly hydrogen bonded to both the anions and the hydroxyl surface. Raman spectroscopy has the advantage that water molecules are not observed as water is a very poor Raman scatterer. Water is however easily measured with infrared spectroscopy. The combination of the two techniques enables the bands ascribed to hydroxyl units and to water molecules to be distinguished. Thus the cation OH stretching vibrations are more readily observed with Raman spectroscopy.

Acknowledgments

The financial and infra-structure support of the Queensland University of Technology Inorganic Materials Research Program is gratefully acknowledged. The Australian Research Council (ARC) is thanked for funding the instrumentation. Ms K. Erickson is thanked for collecting some of the spectra. One of the authors (BJR) thanks the Queensland University of Technology for a Visiting Professorial Fellowship.

References

- [1]. C. Frondel, *Am. Miner.* 26 (1941) 295.
- [2]. M. C. Van Oosterwyck-Gastuche, G. Brown and M. M. Mortland, *Clay Miner.* 7 (1967) 177.
- [3]. C. W. Beck, *Am. Miner.* 35 (1950) 985.
- [4]. J. T. Kloprogge, D. Wharton, L. Hickey and R. L. Frost, *Am. Miner.* 87 (2002) 623.
- [5]. J. T. Kloprogge, R. Evans, L. Hickey and R. L. Frost, *Appl. Clay Sci.* 20 (2002) 157.
- [6]. L. Hickey, J. T. Kloprogge and R. L. Frost, *J. Mat. Sc.* 35 (2000) 4347.
- [7]. R. L. Frost, Z. Ding, W. N. Martens, T. E. Johnson and J. T. Kloprogge, *Spectrochim. Acta* 59 321.
- [8]. R. L. Frost, M. L. Weier, M. E. Clissold, P. A. Williams and J. T. Kloprogge, *Thermochim. Acta* 407 (2003) 1.
- [9]. R. L. Frost and K. L. Erickson, *Spectrochim. Acta, Part A* 60 (2004) 3001.
- [10]. R. L. Frost, M. O. Adebajo and K. L. Erickson, *Spectrochim. Acta, Part A* 61 (2005) 613.
- [11]. Y.-H. Lin, M. O. Adebajo, R. L. Frost and J. T. Kloprogge, *J. Therm. Anal. Calorim.* 81 (2005) 83.
- [12]. J. T. Kloprogge, L. Hickey and R. L. Frost, *J. Raman Spectrosc.* 35 (2004) 967.
- [13]. A. S. Bookin, V. I. Cherkashin and V. A. Drits, *Clays Clay Miner.* 41 (1993) 558.
- [14]. V. A. Drits, N. A. Lisitsyna and V. I. Cherkashin, *Doklady Akademii Nauk SSSR* 284 (1985) 443.
- [15]. V. A. Drits, T. N. Sokolova, G. V. Sokolova and V. I. Cherkashin, *Izvestiya Akademii Nauk SSSR, Seriya Geologicheskaya* (1986) 76.
- [16]. V. A. Drits, T. N. Sokolova, G. V. Sokolova and V. I. Cherkashin, *Clays Clay Miner.* 35 (1987) 401.
- [17]. A. A. Kashaev, G. D. Feoktistov and S. V. Petrova, *Zapiski Vsesoyuznogo Mineralogicheskogo Obshchestva* 111 (1982) 121.
- [18]. W. Martens, R. L. Frost, J. T. Kloprogge and P. A. Williams, *J. Raman Spectrosc.* 34 (2003) 145.
- [19]. R. L. Frost, W. Martens, J. T. Kloprogge and P. A. Williams, *J. Raman Spectrosc.* 33 (2002) 801.
- [20]. R. L. Frost, W. N. Martens and P. A. Williams, *J. Raman Spectrosc.* 33 (2002) 475.
- [21]. R. L. Frost, Z. Ding, W. N. Martens, T. E. Johnson and J. T. Kloprogge, *Spectrochim. Acta, Part A* 59A (2003) 321.
- [22]. R. L. Frost, W. Martens, Z. Ding, J. T. Kloprogge and T. E. Johnson, *Spectrochim. Acta, Part A* 59A (2003) 291.
- [23]. L. Frost Ray, O. Adebajo Moses and L. Erickson Kristy, *Spectrochim. Acta A* 61 (2005) 613.
- [24]. R. L. Frost and Kristy L. Erickson, *Spectrochim. Acta A* 61 (2005) 2697.
- [25]. R. L. Frost and Kristy L. Erickson, *Spectrochim. Acta A* 61 (2005) 51.
- [26]. R. L. Frost and Kristy L. Erickson, *Spectrochim. Acta A* 60 (2004) 3001.
- [27]. R. L. Frost, Weier Matt, E. Clissold Meagan and A. Williams Peter, *Spectrochim. Acta A* 59 3313.
- [28]. R. L. Frost and K. L. Erickson, *J. Therm. Anal. Calorim.* 76 (2004) 217.

- [29]. R. L. Frost, A. W. Musumeci, T. Bostrom, M. O. Adebajo, M. L. Weier and W. Martens, *Thermochim. Acta* 429 (2005) 179.
- [30]. R. L. Frost, A. W. Musumeci, J. Bouzaid, M. O. Adebajo, W. N. Martens and J. T. Kloprogge, *J. Solid State Chem.* 178 (2005) 1940.
- [31]. R. L. Frost, M. L. Weier and J. T. Kloprogge, *J. Raman Spectrosc.* 34 (2003) 760.
- [32]. E. Libowitzky, *Monatshefte fuer Chemie* 130 (1999) 1047.
- [33]. J. Emsley, *Chem. Soc. Rev.* 9 (1980) 91.
- [34]. H. Lutz, *Structure and Bonding* (Berlin, Germany) 82 (1995) 85.
- [35]. W. Mikenda, *Journal of Molecular Structure* 147 (1986) 1.
- [36]. A. Novak, *Structure and Bonding* (Berlin) 18 (1974) 177.
- [37]. E. Libowitzky, *Monatshefte für chemie* 130 (1999) 1047.

List of Figures

Fig. 1 Raman and infrared spectra of the hydroxyl stretching region of manasseite

Fig. 2 ThermoRaman spectra of the hydroxyl stretching region of manasseite

Fig. 3 Raman and infrared spectra of the 1800 to 1100 cm^{-1} region of manasseite

Fig. 4 Raman spectrum of manasseite in the 1100 to 900 cm^{-1} region

Fig. 5 ThermoRaman spectra of manasseite in the 1100 to 900 cm^{-1} region

Fig. 6 Infrared spectra of the 1050 to 550 cm^{-1} region of manasseite

Fig. 7 Raman spectra of the 850 to 250 cm^{-1} region of manasseite

List of Tables

Table 1 Raman and infrared spectral results of natural manasseite

Manasseite					
Raman			Infrared		
Band Centre (cm⁻¹)	FWHM (cm⁻¹)	Intensity (%)	Band Centre (cm⁻¹)	FWHM (cm⁻¹)	Intensity (%)
3589	· 70	· 2.44	3553	· 131	· 2.29
3491	· 114	· 10.39	3456	· 118	· 7.66
3386	· 148	· 14.57	3386	· 160	· 21.76
3255	· 234	· 16.31	3240	· 224	· 17.05
3060	· 200	· 15.07	3036	· 255	· 15.93
2930	· 328	· 14.13	2845	· 212	· 4.38
			2681	· 204	· 1.61
			1750	· 29	· 0.03
			1634	· 117	· 1.67
			1512	· 82	· 1.15
1404	· 49	· 1.03	1447	· 117	· 1.26
			1403	· 52	· 2.88
			1356	· 48	· 6.00
			1346	· 27	· 0.85
1062	· 7	· 4.96	968	· 36	· 0.29
1058	· 16	· 3.14	937	· 52	· 1.11
1035	· 51	· 3.86	870	· 46	· 0.79
958	· 68	· 2.58			
817	· 57	· 0.32	818	· 69	· 2.75
			779	· 46	· 3.30
			752	· 37	· 1.32
696	· 14	· 0.63			
692	· 22	· 0.44	660	· 28	· 0.70
			632	· 41	· 0.61
556	· 11	· 7.60			
551	· 13	· 0.72			
539	· 17	· 0.44			
474	· 44	· 0.26			
396	· 11	· 0.33			
362	· 11	· 0.12			
302	· 10	· 0.15			

Table 1 Results of the Raman and infrared spectra of manasseite

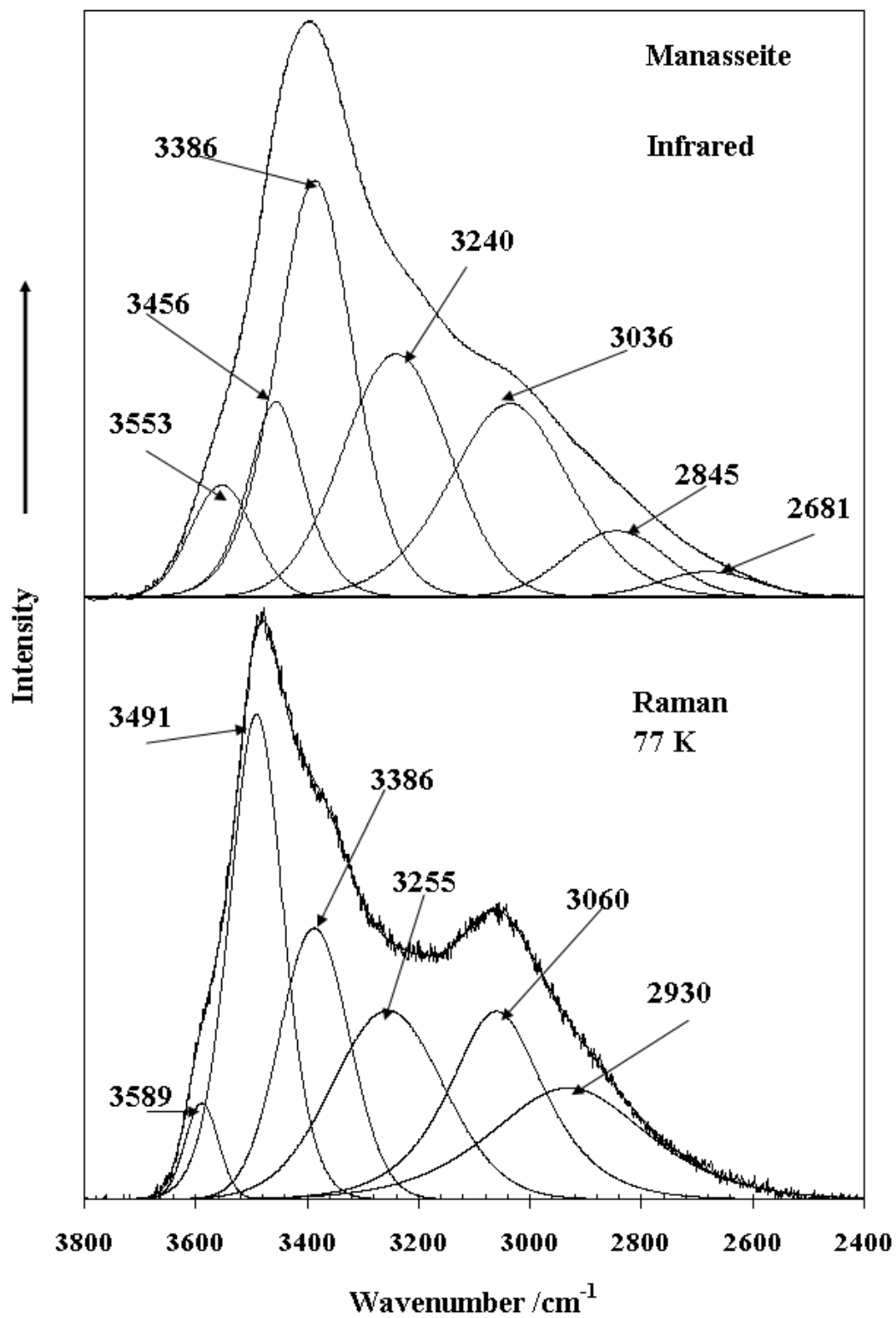


Figure 1

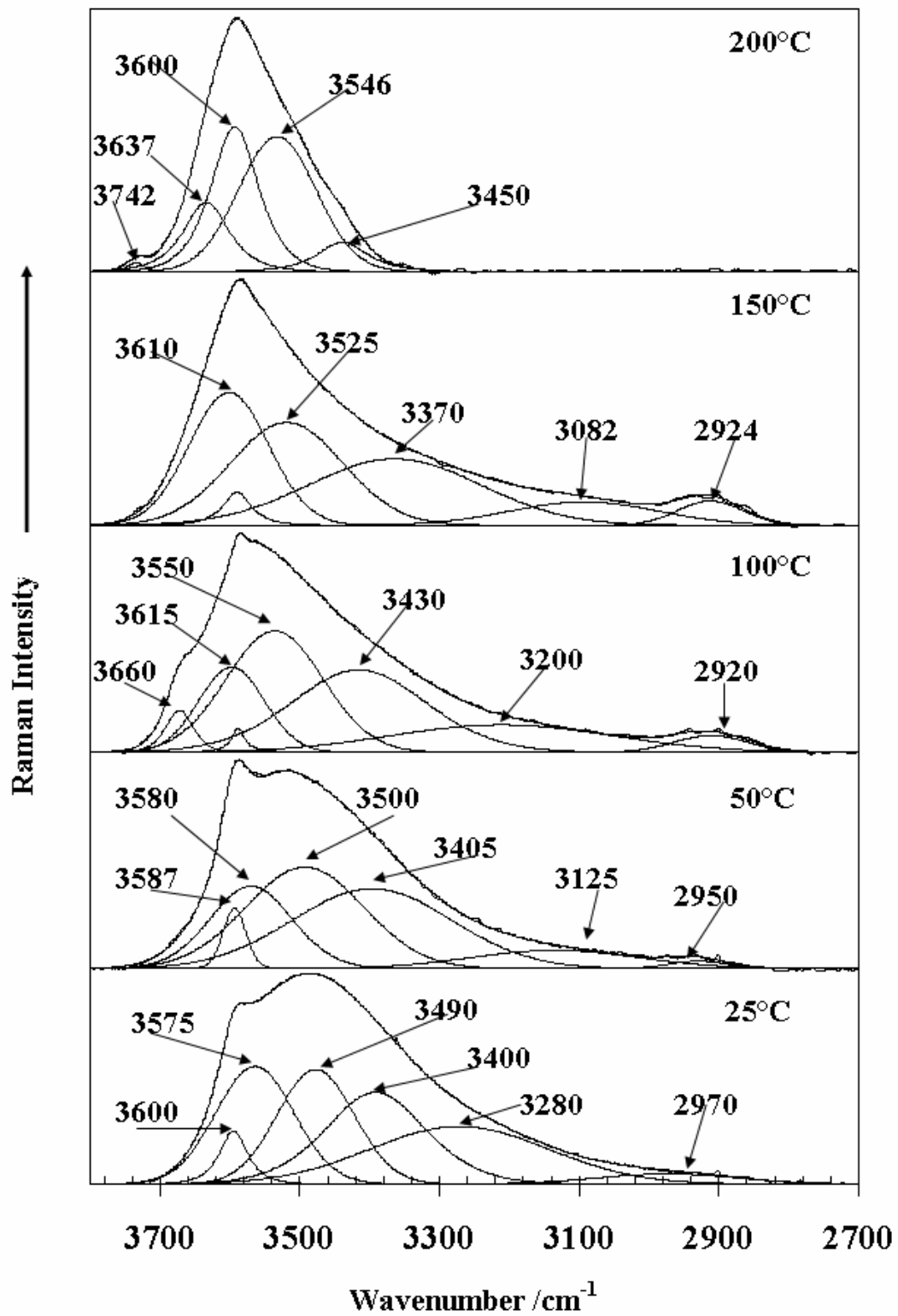


Figure 2.

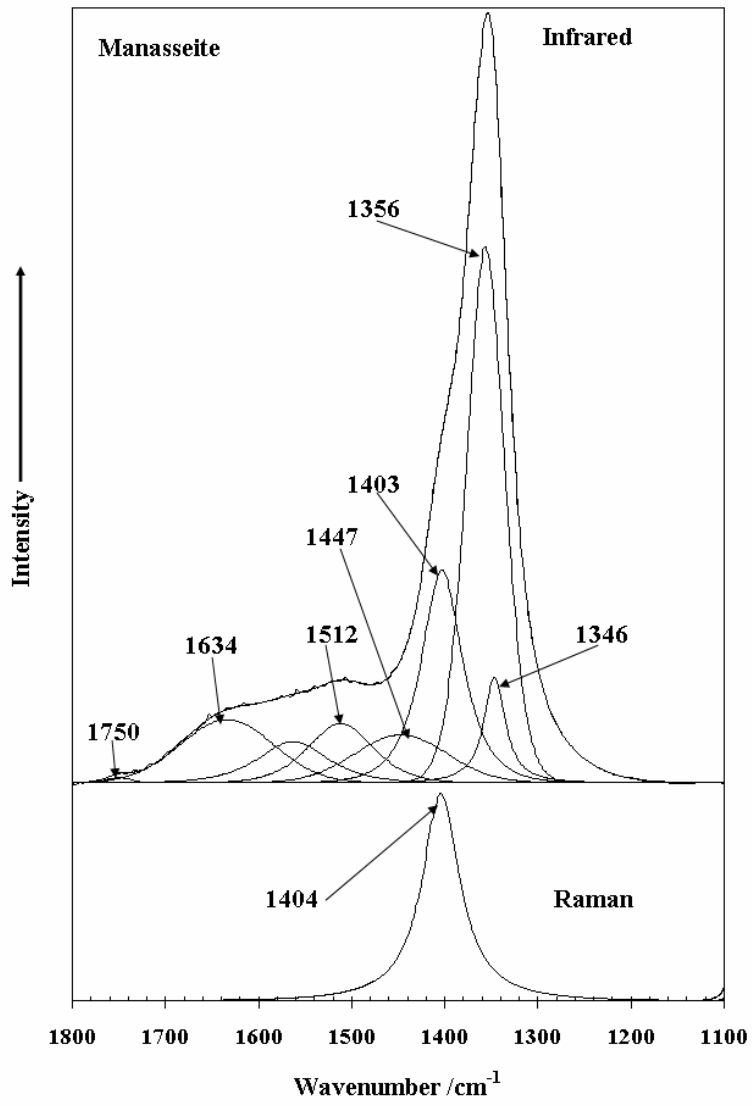


Figure 3

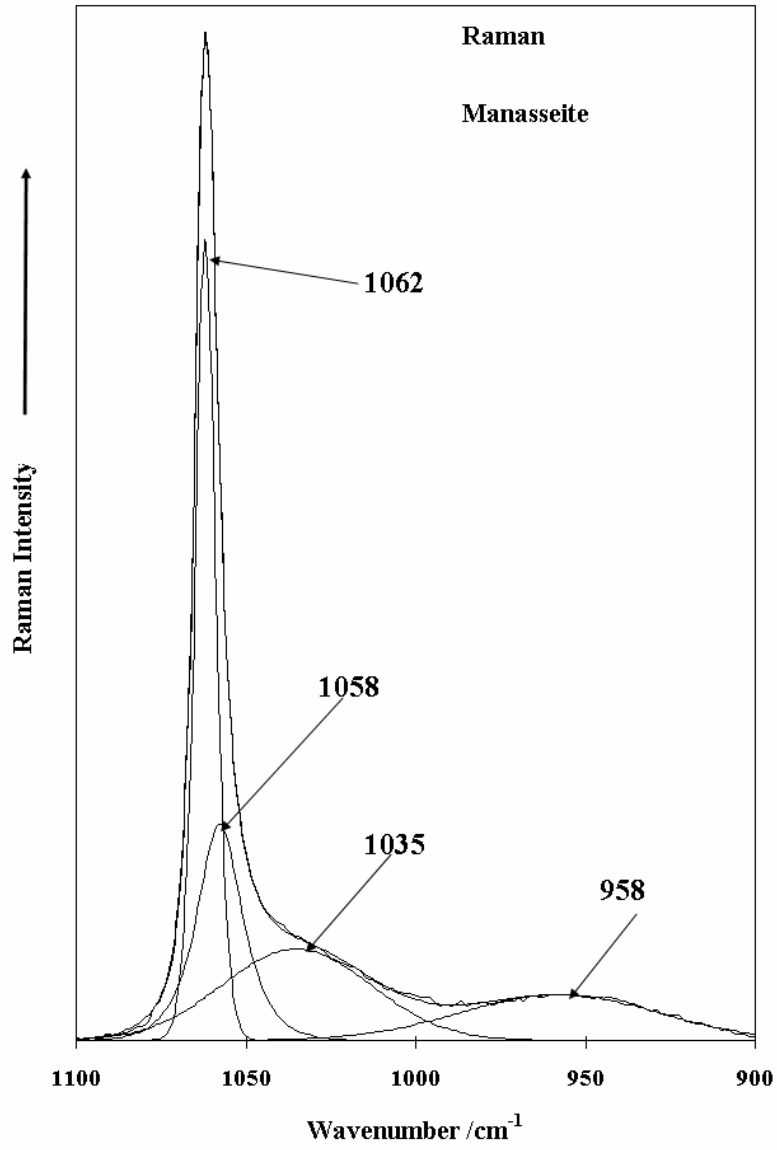


Figure 4

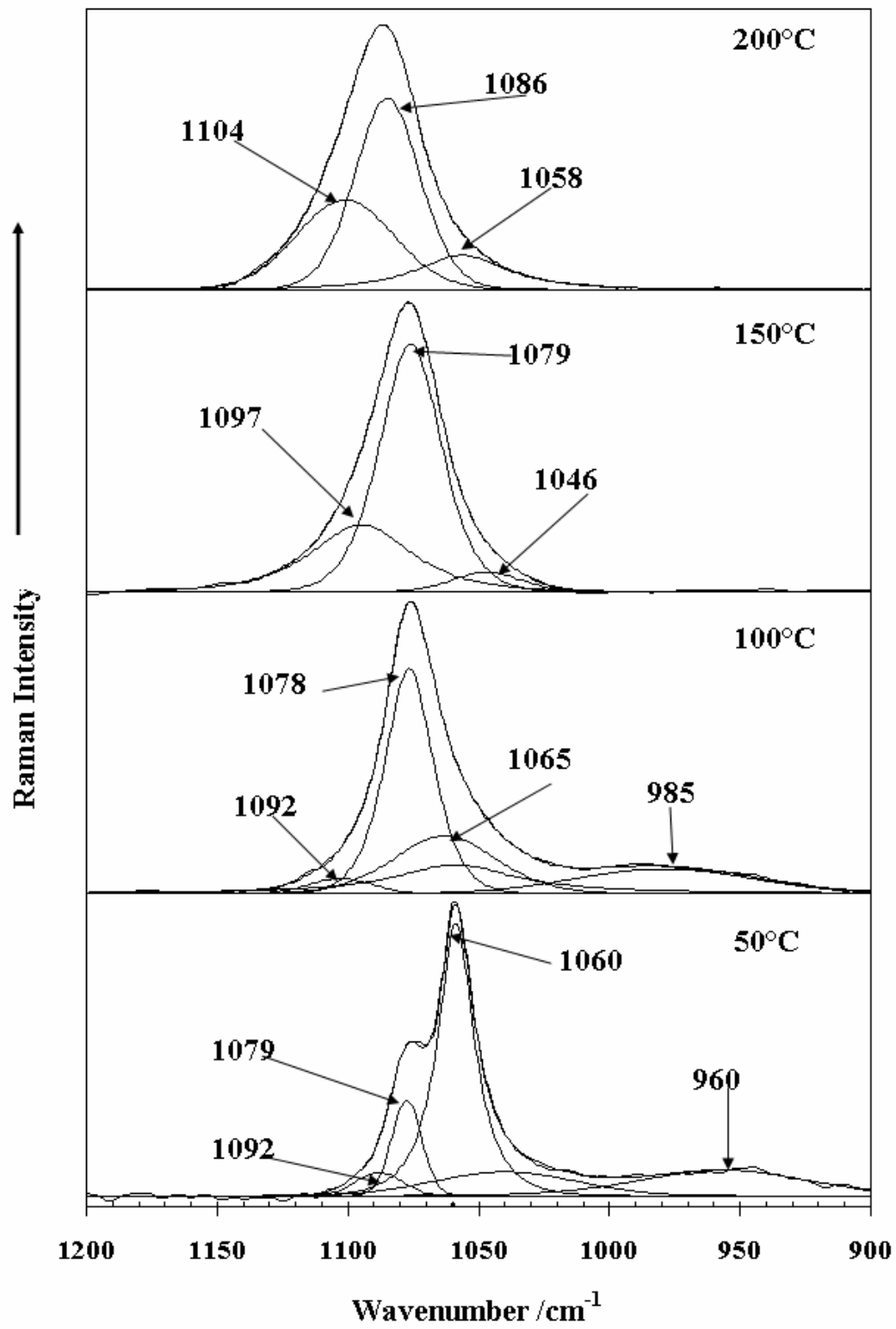


Figure 5

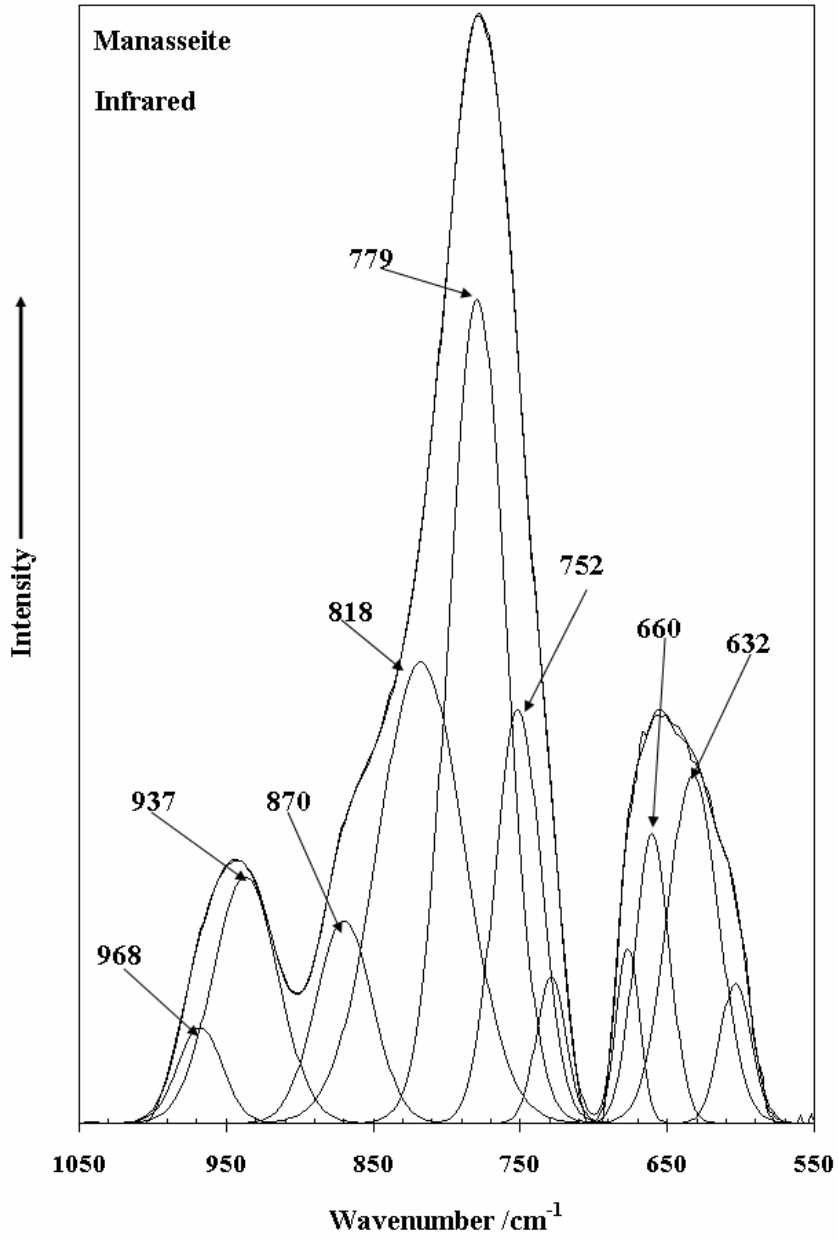


Figure 6

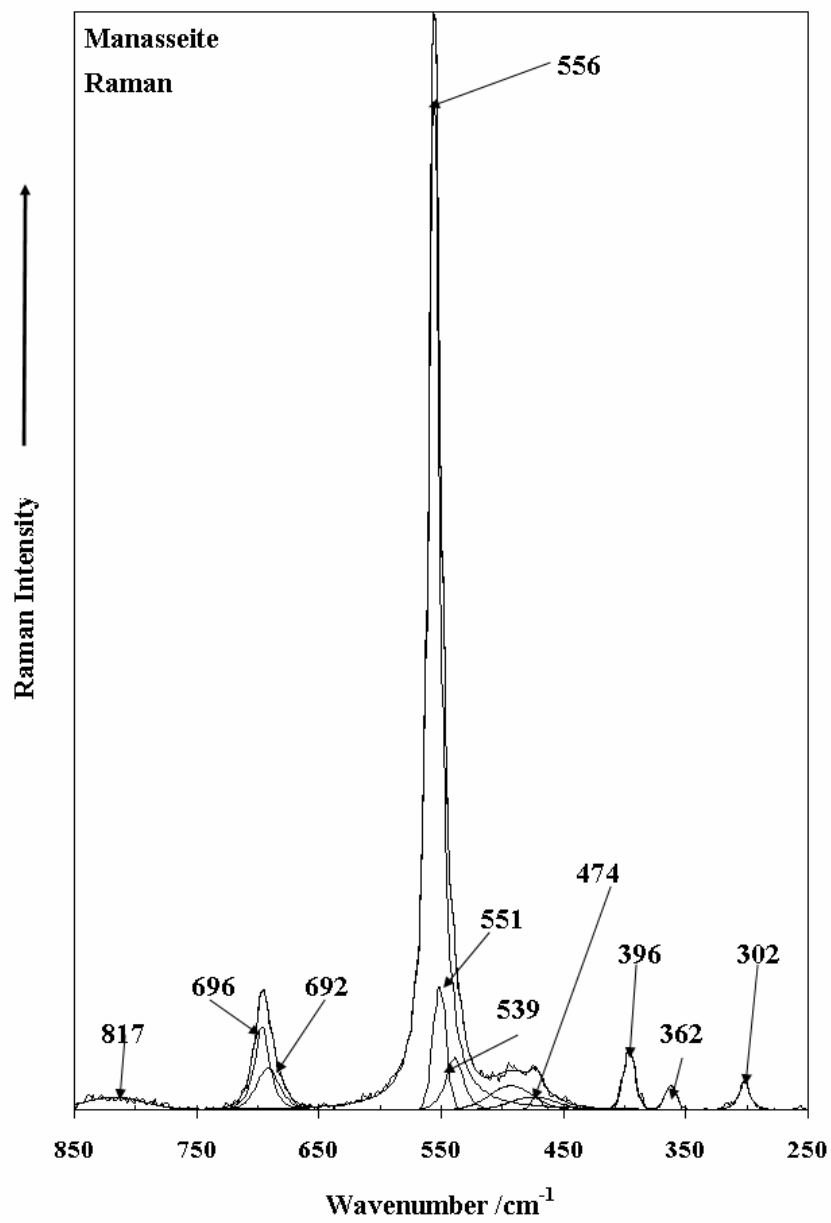


Figure 7